SUPPLEMENTAL MATERIALS

A thromboxane A_2 receptor-dependent feedback loop that affects the homeostasis and angiogenic capacity of endothelial cells

Robert Eckenstaler[§1], Anne Ripperger[§1], Michael Hauke[1], Markus Petermann[1], Sandra Hemkemeyer[2], Edzard Schwedhelm[3], Süleyman Ergün[4], Maike Frye[2], Oliver Werz[5], Andreas Koeberle[5,6], Heike Braun[1] and *Ralf A. Benndorf[1]

§ These authors contributed equally to this work.

[1] Department of Clinical Pharmacy and Pharmacotherapy, Institute of Pharmacy, Martin-Luther-University Halle-Wittenberg, Halle (Saale), Germany

[2] Institute of Clinical Chemistry and Laboratory Medicine, University Medical Center Hamburg-Eppendorf, Hamburg, Germany

[3] Institute of Clinical Pharmacology and Toxicology, University Medical Center Hamburg-Eppendorf, Hamburg, Germany.

[4] Institute of Anatomy and Cell Biology, Julius-Maximilians-University, Würzburg, Germany.

[5] Department of Pharmaceutical/Medicinal Chemistry, Institute of Pharmacy, Friedrich-Schiller-University Jena, Jena, Germany.

[6] Michael Popp Institute and Center for Molecular Biosciences Innsbruck (CMBI), University of Innsbruck, Innsbruck, Austria.

* corresponding author

Expanded Materials and Methods

Reagents, plasmids and siRNAs

All chemicals and reagents were from Sigma-Aldrich (St. Louis, USA), unless stated otherwise. U-46619, SQ 29,548 and blebbistatin were purchased from Cayman Chemical Europe (Tallin, Estland). Recombinant murine and human VEGF-A and bFGF were from PeproTech Inc. (Rocky Hill, USA). The LIMK2 inhibitor LX-7101 was from Lexicon Pharmaceuticals (The Woodlands, USA), the LIMK1 inhibitor BMS4 was from Axon Medchem (Reston, USA), the ROCK inhibitor Y-27632, the COX inhibitors diclofenac and celecoxib as well as the thromboxane A_2 synthase inhibitor ozagrel were from Santa Cruz Biotechnology (Dallas, USA).

Lentiviral plasmids LeGO-C2 and pHIV-SFiG-R1335 were kind gifts of Dr. Boris Fehse (Department of Stem Cell Transplantation, University Medical Center Hamburg-Eppendorf, Germany). For overexpression of the thromboxane A_2 receptor (TP) isoforms TP_α (NP_001051.1) and TP_β (NP_963998.2), the respective codon-optimized coding sequence (CDS) of both transcripts were cloned BamHI and NotI into the pHIV-SFiG-R135 backbone to allow for simultaneous expression of the TP isoforms and the fluorescence reporter enhanced green fluorescent protein (EGFP) in endothelial cells, respectively. To allow for overexpression of wild-type prostacyclin synthase (PTGIS; NP_000952.1), wild-type, untagged PTGIS CDS was cloned into the pHIV-SFiG-R135 backbone. To enable overexpression of dominant negative (T19N-mutated) or constitutively active (Q63L) RhoA (NP_001655.1), 3x-HA-tagged and codon-optimized transcripts of the respective RhoA variants were cloned into the pHIV-SFiG-R135 backbone, respectively. For overexpression of different RhoA mutants and eGFP alone as an adequate transduction control (pHIV-SFiG-1335), HUVEC or HCAEC (passages 2-5) were infected with a multiplicity of infection (MOI) of 500. For shRNA-mediated knockdown of TP (V3LHS_389249 (shTP1), V3LHS_389250 (shTP2)), PTGIR (RHS4430-200220940 (shPTGIR1) and RHS4430-200223542 (shPTGIR2)), $G_{\alpha q}$ (V3LHS_370027) and $G_{\alpha 11}$ (V3LHS_306337) commercially available shRNA sequences as well as a non-silencing shRNA control (RHS4346) pre-cloned into the

GIPZ™ backbone were purchased from Horizon Discovery (Waterbeach, UK). psPAX2 (#12260), and pMD2.G (#12259) plasmids were obtained from addgene (Cambridge, USA). The tension biosensor VinTS (addgene #26019) and its tailless control variant VinTL (addgene #26020), a variant that is incapable of coupling to cytoskeletal adapters of vinculin in vascular endothelial cells, were also obtained from addgene. Generation and validation of both fusion proteins has been published previously [1]. The validated RhoA biosensor [2-4] was kindly provided by Jaap van Buul (Sanquin Research, Amsterdam) and Yi Wu (Uconn Health, Farmington).

Methods

Cell culture

HEK293T cells were grown in 75 cm^2 culture flasks in DMEM high-glucose supplemented with 10% FCS, 1 % penicillin-streptomycin and 1% GlutaMAX (Thermo Fisher Scientific). Primary human umbilical vein endothelial cells (HUVEC), human coronary artery endothelial cells (HCAEC) and human aortic endothelial cells (HAoEC) were purchased from Lonza (Basel, Switzerland) or Promocell (Heidelberg, Germany), respectively. HUVEC were cultured in ready-to-use basal endothelial cell medium (EBM-2, Promocell) supplemented with 2% fetal calf serum (FCS), basic fibroblast growth factor (bFGF), VEGF-A, insulin-like growth factor-1 (IGF-1), epidermal growth factor (EGF), hydrocortisone, ascorbic acid, gentamycin sulfate and amphotericin-B at 37°C in humidified air with 5% CO_2. HCAEC were grown accordingly in basal endothelial cell medium (MV-2) containing VEGF-A, bFGF, EGF, IGF-1, hydrocortisone, ascorbic acid and 5% FCS. HAoEC were cultured on bovine fibronectin-coated (Sigma-Aldrich Cat. F1141, used at 1 µg/mL diluted in DPBS) dishes in complete endothelial cell growth medium MV (PromoCell). Cells in passages 2-7 were used for experimental procedures, i.e. transfection and lentiviral transduction procedures as well as consecutive proliferation, angiogenic sprouting, tube formation, migration, trans-well migration, flow experiments, and xenograft implantation assays.

Production, purification and titer determination of lentiviral vectors

Production, purification and titration of lentiviral vectors was performed as described previously [5, 6]. In brief, HEK293T cells were seeded in 150 cm^2 dishes at a density of $8x10^6$ cells per dish in DMEM high-glucose medium supplemented with 10% FCS, 1 % penicillin-streptomycin and 1% GlutaMAX. After 24 h, the cells reached 30-40% confluence and were used for transfection. Two helper plasmids (21 µg pMD2.G (VSV-G envelope-expressing plasmid); 39 µg psPAX2 (2nd generation lentiviral packaging plasmid)) and the transfer vector (60 µg) were mixed with 2 M $CaCl_2$, water and 2x HBS at pH 7.07. Right before transfection, chloroquine in a final concentration of 25 µmol/L was added to the medium. An amount of 6 ml of the DNA/$CaCl_2$/HBS mixture was added dropwise to each dish. After 20 h, medium was changed once. Two days after transfection, the cell supernatant was collected, centrifuged (500xg; 10 min) and filtered (0.45 µM). For lentiviral particle concentration, the filtered supernatant was mixed with 50 % polyethylene glycol 6000 (PEG 6.000), 4 M NaCl and 1x phosphate-buffered saline (PBS). The mixture was kept at 4 °C for 1.5 h. The bottles were shaken slightly every 20-30 min. After centrifugation (7,000xg, 10 min, 4 °C), the pellets were resuspended in 50 mM Tris-HCl, pH 7.4, and stored at -80°C.

Lentiviral vector titers were estimated by flow cytometry. For this purpose, 30,000 endothelial cells per well were plated in 12-well plates (Greiner, Kremsmünster, Germany). 48 h post-transduction with a known amount of virus suspension, cells were harvested and washed twice with 10% FCS in PBS. The quantity of EGFP-positive cells was analyzed by FACS (Attune® Acoustic Focusing flow cytometer; Thermo Fisher Scientific, Waltham, USA). The virus titer was calculated according to the following equation: Transducing units (TU) mL-1=(F*N*D*1000)/V, where F is the percentage of fluorescent cells, N is the number of cells at the time of transduction, D is the fold dilution of virus used for transduction and V is the volume of diluted virus added per well at transduction.

Lentiviral transduction of human endothelial cells

For generation of fluorescent reporter-expressing HUVEC, cells (passages 2-4) were infected with VSV-G-pseudotyped lentiviral particles derived from the LeGO-C2 (red fluorescent protein mCherry) or pHIV-SFiG-1335 (EGFP) transfer plasmids, respectively. For TP or PTGIS expression (pHIV-SFiG-1335 vectors) or shRNA-mediated knockdown (GIPZ™ vectors) of TP downstream effectors, HUVEC and HCAEC were again infected with the corresponding lentiviral particles. Unless stated otherwise, the lentiviral transduction of endothelial cells was performed with a multiplicity of infection (MOI) of 100. Infected cells were cultivated for at least 48 h prior to functional and/or gene expression analyzes. In all knockdown and overexpression experiments, knockdown efficiencies or overexpression levels were determined by real-time PCR or Western Blot analyzes, respectively. Lentiviral transduction efficiencies were additionally assessed by detecting the fraction of EGFP-expressing endothelial cells (usually exceeding 90%).

Angiogenic sprouting (endothelial cell spheroid) assay *in vitro*

Analyses of angiogenic sprouting from endothelial spheroids were carried out as described by Korff and Augustin, 1998 [7]. Briefly, HUVEC were resuspended in endothelial growth medium containing 20% methocel and were seeded dropwise into non-adherent culture dishes and allowed to form endothelial aggregates (spheroids) overnight in “hanging drops” containing 600 cells each at 37°C in humidified air with 5% CO_2. In knockdown experiments, siRNA-treated HUVEC were seeded for 24 h after the transfection procedure prior to spheroid formation. For live cell imaging of angiogenic sprouting, spheroids consisting of equal amounts of GFP- and mCherry-expressing cells were generated. Subsequently, 500 spheroids were embedded in 1000 µL of rat collagen containing 20% methocel and 10% FCS in non-adhesive 24-well plates and kept in basal endothelial medium with or without VEGF (20 ng/mL) in presence or absence of pharmacological blockers for at least 24 h. Angiogenic sprouting was quantified by measuring the cumulative sprout length of each

spheroid using the NIS elements digital imaging software (Nikon, Tokyo, Japan), analyzing 10 spheroids per experimental group and experiment.

Endothelial tube formation assay

For assessment of endothelial tube formation, growth factor–reduced matrigel (Corning Life Sciences, Wiesbaden, Germany) was placed in 96-well angiogenesis µ-Plates (10 µL/well; Ibidi, Munich, Germany) and allowed to gel at 37°C for 30 minutes. Then 2 x 10^4 HUVEC were added to each well and incubated in EBM-2 (Promocell) supplemented with 2% FCS at 37°C for 24 h in humidified air with 5% CO_2. Tube length and morphological changes were visualized using an epifluorescence microscope (Nikon). The total tube length was measured at 10x magnification using the NIS elements software (Nikon).

Live cell imaging of endothelial cell migration and angiogenic sprouting

Live cell imaging was performed using a Nikon A1R confocal microscope (Nikon) carrying lasers at 405, 457-514, 561, and 642 nm equipped with an O_2/CO_2 okolab cage incubator (okolab, Ottaviano, Italy). Time-lapse images of angiogenic sprouting from endothelial "mosaic" spheroids equally composed of EGFP- and mCherry-expressing HUVEC, respectively, were captured at 20 min intervals for up to 36 h using a CFI Plan Apochromat 10x objective (Nikon). To visualize the effect of TP upregulation on angiogenic sprouting of HUVEC, spheroids were kept with VEGF (20 ng/mL). The mosaic spheroid setup was chosen to allow for monitoring of different behaviour of TP-overexpressing HUVEC (also expressing the fluorescent reporter EGFP) during direct interaction with phenotypic "normal" mCherry-expressing control cells. In analogous setups, EGFP- and mCherry-expressing HUVEC were used to analyze the effect of TP overexpression on two-dimensional endothelial cell migration. For this purpose, control and TP overexpressing HUVEC were seeded at a density of 1500 cells/well in 96-well plates in basal endothelial cell medium. All analyzes of time-lapse image series (including migration distance and speed) were performed using the NIS elements software package (Nikon).

Scratch assay / wound healing assay

Scratch-related endothelial cell migration was investigated with living HUVEC and HCAEC using the scratch (wound healing) assay and time-lapse microscopy as described previously [8]. Briefly, 5,000 cells/well were seeded in a gelatine-coated 96-well plate, transduced with lentiviral vectors and grown to confluence for 72 hrs. Then, a wound was set creating a gap in which cells could migrate. During the course of the experiment, cells were incubated in basal endothelial growth medium supplemented with 2.5% FCS. Cell movement was imaged in TP knockdown as well as in TP-overexpressing and appropriate control cells at 20 min intervals for up to 24 h. The analyses of TP-overexpressing human endothelial cells were performed in presence or absence of VEGF (20 ng/mL), the TP antagonist SQ 29,548 ($3x10^{-5}$ mol/L), the TP agonist U-46619 ($3x10^{-5}$ mol/L), the COX-2 inhibitor celecoxib (100 nmol/L), the ROCK inhibitor Y-27632 (10 µM), the LIMK1 inhibitor BMS4 (0.5 µM), the LIMK2 inhibitor LX-7101 (3 µM) or the myosin II inhibitor blebbistatin (30 µM). These analyses were performed using the CFI Plan Apochromat 10x objective. Analyses of time-lapse image series, were performed using the NIS elements software package (Nikon).

Trans-well cell migration assay

Trans-well cell migration assays were performed using a 96-well Boyden chemotaxis apparatus (Neuroprobe; Cabin John, MD). Briefly, polycarbonate membranes with a pore size of 8 µm (Neuroprobe) were coated with 5% solution of type I collagen diluted in 0.1% acetic acid, overnight, washed with phosphate buffered saline supplemented with 1% FCS and equilibrated with HUVEC basal medium containing 2% FCS. The membranes were placed on the lower chambers of the chemotaxis apparatus which contained test samples (20 ng/mL VEGF, 10% FCS with or without 30 µM SQ 29,548). Lentiviral transduced HUVEC (Ctr., TP_α, TP_β) were trypsinized with 0.05% trypsin/ EDTA and washed in PBS. $2x10^4$ cells were suspended in 50 µL basal endothelial medium with 1% FCS and were pipetted into each upper chamber. The filled apparatus was incubated for 5 h at 37 °C in humidified air with 5% CO_2. After incubation, the filter was removed from the apparatus and cells were fixed

with methanol and stained with eosin (Roth) and haematoxylin (Roth). Non-migrated cells were removed from the upper surface of the insert with a cotton swab. Total membranes were imaged by colour microscopy and the amount of migration was expressed as percentage of area of stained cells / total membrane area normalized to control.

Live cell detection of endothelial cell tension (VinTS) as well as RhoA activity using FRET-based biosensors and live-cell actin staining.

HUVEC were plated in a 96-well glass bottom plate (Greiner) coated with 50 µg/mL fibronectin (Santa Cruz Technology, Dallas, USA) at a density of 10,000 cells per well and transfected with fluorescent FRET biosensors (VinTS, VinTL, RhoA WT, RhoA Pos., RhoA Neg.) using the TurboFect reagent (Thermo Fisher Scientific) according to the manufacturer`s recommendations. In further experiments, endothelial cells were transduced with lentiviral (EGFP-defective) TP_{α}, TP_{β} or control vectors prior to transfection with the FRET biosensors. Time-lapse FRET imaging was performed at 37°C using a Nikon A1R confocal microscope equipped with a 60x oil immersion objective (plan apo lambda, Nikon, n.a.=1.4), an argon laser (Melles Griot, Germany), a PMT/GaAsP detector unit (Nikon) and an O_2/CO_2 cage incubator (okolab, Ottaviano, Italy). Images were acquired and processed using the NIS-Elements FRET module (Nikon). The FRET donor (VinTS: mTFP1, RhoA: mCerulean3) were exited using the 457 nm laser line (argon laser) and fluorescence emission was detected in the spectral range of the donor (465-500 nm, DD image) and the acceptor (525-555 nm, DA image), respectively. In addition, the FRET acceptor (mVenus) was exited using the 514 nm laser line (argon laser) and detected in the spectral range of the acceptor (525-555 nm, AA image). Laser power and detector gain were set in a way to obtain best signal intensities while avoiding oversaturation of the images. Image settings were kept constant for each series of measurement and each image measured during subsequent time-lapse recordings. Calculation of FRET index was calibrated using donor and acceptor only samples (RhoA: mCerulean3, mVenus / VinTS: mTFP1, mVenus) to determine the correction factors for donor crosstalk (α) and the acceptor's direct excitation (β) in the DA

image. Images displaying the color-coded FRET index were calculated as intensity of the corrected FRET image normalized by the intensity of the donor image according to the following formula (FRET index = 100% * (DA – αDD –βAA) / DD). For live-cell actin staining, HUVEC were stained with 1 µM SiR-actin (Cytoskeleton Kit, Spirochrome, Switzerland) in HUVEC medium for 1 h at 37 °C and 5% CO_2. Fluorescence of SiR-actin staining was excited using a 638 nm laser line (diode laser, Melles Griot, Germany) and monitored in the detector range of 663-738 nm.

Immunocytochemistry

HUVEC were transduced with lentiviral particles (Ctr., TP_α, TP_β). After 24 h, cells were passaged and seeded at a density of 50,000 cells / well on gelatine-coated glass coverslips placed in a 24-well plate. The next day, cells were transfected with vinculin tension sensor (VinTS) using the TurboFect reagent (Thermo Fisher Scientific) according to the manufacturer`s recommendations. 24 h after transfection, cells were fixed in 4% PFA in PBS for 5min and permeabilised in 0.1% Triton X 100 (Roth) in PBS for 10min at room temperature. After blocking (10% normal goat serum, Cell Signaling; 1% BSA, Roth, 0.1% Tween 20, Roth) for 1 h at room temperature, cells were stained with primary rabbit monoclonal paxillin antibody (ab32115, Abcam) diluted 1:100 (=1.17 µg/mL) in SignalStain ab diluent solution (Cell Signaling) and incubated for 2 h at 4°. Secondary antibody (Alexa Fluor 594 conjugated donkey-anti-rabbit, Jackson ImmunoResearch Laboratories) was diluted 1:100 in SignalStain ab diluent solution (Cell Signaling) and incubated for 1 h at room temperature. Hoechst 33342 (life technologies) was diluted 1:1,000 and incubated for 5min at room temperature. Coverslips were mounted on glass slides using SignalStain mounting medium (Cell Signaling).

Image Processing

NIS Elements (Nikon) and Photoshop CS2 (Adobe, San José, USA) were used for image processing according to the AHA/ASA Journal Image Preparation Guidelines. In order to

improve the visibility of fluorescence structures, brightness and contrast were uniformly increased over the entire image and the settings made were then applied identically to the image material of all experimental groups in one experiment. In the case of time-lapse imaging to compare morphological changes of fluorescent structures whose fluorescence intensities depend on the degree of transgene expression of the cell, image display was adapted so that comparable structures were similarly visible. The settings were then retained for each subsequent image during time-lapse imaging. In kymograph presentations, a representative 10x200 pixel portion of each time-lapse image was cut out and lined up one after the other to visualize changes over time in this region. For multicolor merged images, the contrast and brightness of the individual color channels were adjusted to optimize their visibility.

Endothelial cell proliferation analysis

Proliferation of TP-regulated human endothelial cells (HUVEC) was analyzed by flow cytometry (Attune® Acoustic Focusing Flow Cytometer) after cells were seeded on gelatin-coated 24-well plates (Greiner) and grown for up to 72 hours in commercial growth medium (Promocell). 72 hours prior to seeding, cells were infected with the appropriate lentiviral particles with a MOI of 500 for either TP overexpression (pHIV-SFiG-1335 vectors) or shRNA-mediated knockdown of the TP (GIPZ™ vectors). Subsequently, 12,500 HUVEC per well were plated, grown as described above, and detached by trypsinization 2 h, 24 h, or 72 h after plating. To some TP-overexpressing HUVEC subgroups, the pharmacological TP inhibitor SQ 29,548 was added at a concentration of $3x\ 10^{-6}$ mol/L after plating to check for reversibility of the effect induced by TP overexpression. Lastly, detached HUVEC were measured by flow cytometry, counting only GFP-positive (i.e., successfully transduced) HUVEC.

The proliferation behaviour of TP-regulated endothelial cells was additionally analysed by the BrdU (5-bromo-2´-deoxyuridine) incorporation assay and by immunofluorescence staining of the nuclear proliferation marker Ki-67. These are two well-established biomarkers of cell

proliferation, which, however, do not directly measure cell proliferation. Incorporation of BrdU in newly synthesized cellular DNA was investigated with a commercially available cell proliferation ELISA (Roche, Basel, Switzerland) according to the manufacturer's instructions. Briefly, 2.500 cells/well were seeded in a 96-well plate (Greiner) and infected with the appropriate virus 24 h after seeding. BrdU incubation was done 72 h post-infection for 3 h at 37°C. Afterwards, cells were fixed, denatured and incubated for 90 min with BrdU antibody. Following the manufacturer´s instructions, samples were washed with 1x PBS and peroxidase substrate solution was added. Read-out was done by adding 1 M H_2SO_4 to each well to stop the peroxidase reaction and measuring the absorbance at 450 nm with a Tecan infinite F200pro plate reader (Tecan, Männedorf, Switzerland). For Ki-67 staining, endothelial cells were cultured and processed as described in other sections (see section "Immunofluorescence staining and confocal laser-scanning microscopy"). After fixation, blocking and permeabilization (3% BSA, 0,2% Tween 20, 2% Triton X-100 in 1x TBS), cover slips were incubated in a humidified chamber overnight at 4°C with a mouse monoclonal Ki-67 antibody (1:400 = 557.5 ng/mL, #9449, Cell Signaling Technology, Danvers, USA) in Signal Stain (R) Ab Diluent (Cell Signaling Technology). Afterwards, cells were incubated with an AlexaFluor594-conjugated goat anti-mouse antibody (1:1,000; Dianova, Hamburg, Germany) and Hoechst 33342 (1 mg/mL) to visualize Ki-67 and nuclei, respectively. After washing with 1x PBS, cover slips were mounted in Dako Fluorescence Mounting Medium (Agilent, Santa Clara, California, USA) and analyzed using a Nikon A1R confocal microscope (Nikon).

Endothelial flow experiments

For flow experiments, ibiTreat µ-slides Luer (Ibidi Cat. 80186) were coated with fibronectin (as described above), HAoEC were trypsinized and cell suspension adjusted to $1.6x10^6$ cells/mL. 80 µl cell suspension were seeded into the channel of the fibronectin-coated µ-slides after removing coating solution. 100 µl additional culture medium was added per reservoir after cells had properly attached. Cells were allowed to adhere for 24 h before

being subjected to a laminar flow of 10 dyn/cm^2 for 24 h employing the ibidi Pump System (Ibidi Cat. 10902 with Perfusion Set RED Cat. 10962). As static controls, HAoEC were similarly seeded in a µ-slide and left for 24 h without flow application.

Western Blot analysis

Western blot analysis of cellular protein levels was performed as previously described [9, 10]. In brief, endothelial cells were lysed using pre-made lysis buffer (Cell Signaling Technology) containing 20 mmol/L Tris/HCl, pH 7.5, 1 mmol/L Na_2EDTA, 1mmol/L EGTA, 150 mmol/L NaCl, 1% Triton X-100, 2,5mmol/L $Na_4P_2O_7$, 1mmol/L b-glycerophosphate, 1 mM Na_3VO_4, and 1 µg/mL leupeptin and a premade protease and phosphatase inhibitors single use cocktail (Thermo Fisher Scientific). The lysates were subsequently centrifuged for 5 min, 4°C, at 1500xg to remove cell detritus. Equal amounts of proteins (30 µg/lane) were separated by SDS-PAGE and transferred to a nitrocellulose membrane. Afterwards, membranes were incubated with appropriate primary antibody solution and anti-β-Actin (clone AC-15) for normalization (Sigma Aldrich; 1:5,000 = 420ng/mL). Antibodies directed against the TP_α and TP_β isoform were purchased from Cayman Chemical (TP_α; #10004452; 1:500) and Genscript (custom-made NP963998; 1:500). Bound antibodies were detected by peroxidase-conjugated secondary antibodies and the ECL system (Amersham Bioscience, Amersham, UK).

Real time RT-PCR

Total RNA was isolated, reverse transcribed and analyzed as described previously [11, 12]. mRNA expression was quantified using the ABI 7500 Real-Time PCR System (Thermo Fisher Scientific). TaqMan reactions were carried out in 96-well plates according to the manufacturer's instructions using pre-made probes for the AQP1 (Hs01028916_m1), CXCL8 (Hs00174103_m1), COX-2 (Hs00153133_m1), $G_{\alpha q}$ (Hs00387073_m1), $G_{\alpha 11}$ (Hs01588833_m1), HDAC9 (Hs01081558_m1), ITGB4 (Hs00236216_m1), MYLK (Hs00364926_m1), PTGIS (Hs00919949_m1), PTGIR (Hs01125026_m1), TP

(Hs00169054_m1; Mm00436917_m1), VEGFR-2 (Hs00911700_m1). Hypoxanthine-guanine phosphoribosyltransferase 1 (HPRT1) was used as an endogenous control (Hs02800695_m1; Mm01545399_m1). We performed relative quantification of gene expression using the delta-delta Ct method [13].

Site-directed mutagenesis

To enable lentiviral overexpression of the TP_α or TP_β isoform, respectively, in the absence of simultaneous EGFP expression, a stop codon was inserted by site-directed mutagenesis into the sequence opening of the EGFP CDS contained in the pHIV-SFiG-R135 backbone to generate EGFP stop variants of pHIV-SFiG-R135 control as well as of the pHIV-SFiG-R135-TP_α and pHIV-SFiG-R135-TP_β vectors, respectively. Site-directed mutagenesis was performed as described previously [14] using the QuickChange® Lightning Site-Directed Mutagenesis Kit (Agilent Technologies, Santa Clara, USA) with specific primers according to the manufacturer's instructions. The sense primer for the EGFP stop mutation was synthesized as follows: *5`-CACAACCATGGTGAGCTAGGGCGAGGAGCTGTTC-3`*. Successful mutagenesis was verified by sequencing (Microsynth Seqlab, Göttingen, Germany).

RNA sequencing and differential gene expression analyzes

Total RNA was isolated from control or TP-overexpressing HUVEC using the TRIZOL™ reagent (Thermo Fisher Scientific) according to the manufacturer's recommendations. RNA integrity and size distribution were tested with a Bioanalyzer 2100 (Agilent Technologies, Santa Clara, USA) and by agarose gel electrophoresis. For library preparation, 1 µg RNA per sample served as input. RNA-seq libraries were generated using NEBNext® Ultra™ RNA Library Prep Kit for Illumina® (New England BioLabs, Ipswich, USA) following the manufacturer's recommendations and were sequenced by the Novogene Bioinformatics Institute (Beijing, China) as 150-bp paired-end reads on an Illumina Novaseq 6000 platform. The quality of raw reads was first assessed using Novogene in-house scripts. Clean reads were used in the future steps after removing low quality, adapter and poly-N from raw data.

Reads were aligned to the human genome (GRCh38) with HiSat2 (v2.0.5) [15]. Ensembl (GRCh38.p13) was used for annotations [16]. The read numbers mapped to each gene were determined with HTSeq (v0.6.1) [17] and subsequently Fragments Per Kilobase of transcript per Million mapped reads (FPKM) of each gene was calculated based on gene length and read counts mapped to the respective gene. Differential gene expression analysis was performed using the DESeq2 software package (v1.20.0) [18]. Resulting *p*-values were adjusted using the Benjamini and Hochberg approach to control the false discovery rate (FDR). Genes with an adjusted $p<0.05$ were classified as differentially expressed. Gene Ontology (GO) pathway enrichment analyzes were performed using the GOseq R software package (v1.34.1) [19]. GO terms with an adjusted $p<0.05$ were considered significantly enriched. Hierarchical clustering of differentially expressed genes was performed with FPKM values as the input in pheatmap package by clustering rows and columns in R.

Prostanoid profiling in HUVEC by UPLC-MS/MS

Lipid mediators were extracted from HUVEC kept in EBM2 (5 ml, Lonza) and cell culture supernatant by adding ice-cold methanol (10 ml) containing the internal standards d_8-5*S*-HETE and d_4-PGE_2 (Cayman Chemicals, Ann Arbor, USA). Solid phase extraction and UPLC-MS/MS analysis were conducted as previously described [20, 21]. In brief, proteins were precipitated at -20°C for 60 min and removed by centrifugation (1,200×g, 4 °C, 10 min). The supernatants were diluted in water (15 ml), acidified to pH 3.5, and loaded onto solid-phase cartridges (Sep-Pak® Vac 6 cc 500 mg/ 6 ml C18; Waters, Milford, USA). After washing with water and *n*-hexane, lipid mediators were eluted with methyl formate and evaporated to dryness (TurboVap LV, Biotage, Uppsala, Sweden). Extracted lipid mediators were dissolved in methanol/water (50/50) and separated on an Acquity™ UPLC BEH C18 column (1.7 µm, 2.1 × 100 mm; Waters) using an Acquity™ UPLC system (Waters). The UPLC system was coupled to a QTRAP 5500 mass spectrometer (Sciex, Darmstadt, Germany), which was equipped with a Turbo V™ electrospray ionization source and operated in the negative ion mode to analyze lipid mediators by multiple reaction monitoring. Prostanoids and 11-HETE

were characterized by their retention time and at least six diagnostic ions. Quantification is based on calibration curves of external standards (Cayman Chemicals) [21]. In variation to the settings described above, 6-keto-$PGF_{1\alpha}$ was analyzed by UPLC-MS/MS as previously described [22].

Flow cytometry

Quantification of COX-2 (PTGS2), VEGFR-2, and DLL4 protein content was performed by flow cytometry with fixed and permeabilized (BD Cytofix/Cytoperm™ Fixation/Permeabilization Solution Kit; BD Biosciences, Franklin Lakes, USA) endothelial cells using a PE-conjugated mouse monoclonal anti-COX-2 antibody (clone AS67) (BD Pharmingen, San Diego, USA; 1:50 = 2 µg/mL). As isotype control antibody, mouse IgG1, κ Isotype Ctrl. (Biolegend, 2 µg/mL) was used. Moreover, endothelial cells were incubated with PE- or APC-conjugated anti-VEGFR-2 (clone 7D4-6) or DLL4 (clone MHD4-46) antibodies for 20 min on ice for simultaneous detection of VEGFR-2 and DLL4 (Biolegend, San Diego, USA; 1:100, = 2 and 4 µg/mL, respectively). After the staining procedure on ice for 20 min, cells were washed three times with 1x cell staining buffer (Biolegend) and analyzed using an Attune® Acoustic Focusing flow cytometer (Thermo Fisher Scientific). In TP-overexpressing cells, the GFP-positive subset was analyzed and compared to GFP-positive control endothelial cells. Flow cytometric data were analyzed and plotted using the FlowJo software package (Tree Star Inc., Ashland, USA) [23].

Animals

Generation of conditional TP knockout mice has been described previously [24]. These mice were obtained from The Jackson Laboratory (Bar Harbor, USA; stock #021985). To generate mice with specific deletion of the TP in the vascular endothelium, floxed homozygous mice were crossed to Tie2-cre mice [25] previously obtained from The Jackson Laboratory (stock #004128). The resultant mice were bred to generate floxed homozygous mice. In this study, male and female vascular endothelial TP-deficient mice (Tie2-cre-positive) as well as sex-

matched wild-type (Tie2-cre-negative) littermates aged 11 to 13 weeks were studied. All HUVEC spheroid grafting analyzes were performed in female and male NOD-scid IL2rg^{null} (NSG^{TM}) mice that carry two mutations on the NOD/ShiLtJ genetic background: severe combined immune deficiency (Prkdc^{scid}) and a complete null allele of the IL2 receptor common gamma chain (IL2rg^{null}) [26]. These mice were obtained from The Jackson Laboratory (stock # 005557). In this study, NSG^{TM} mice aged 11 to 16 weeks were used.

Isolation of mouse lung endothelial cells (MLECs)

For MLECs isolation, vascular endothelial TP-deficient mice (Tie2-cre-positive) and wild-type (Tie2-cre-negative) mice were killed by cervical dislocation. Lungs were harvested and dissociated by using the mouse lung dissociation kit (Miltenyi Biotec, Bergisch Gladbach, Germany), according to the manufacturer's protocol. Afterwards, endothelial cells were isolated by magnetic cell sorting (Miltenyi Biotec). For the enrichment of CD31+ endothelial cells, lung cells were incubated with CD31 microbeads. mRNA derived from CD31+ cell fractions were analyzed by real-time RT-PCR.

***In vivo* angiogenesis assays**

All animal experiments were carried out in accordance with the directive 2010/63/EU and the German law (Tierschutzgesetz). The experiments were ethically and legally approved by the governmental, local animal committee (approval numbers 42502-2-1418 MLU and 42502-2-1419 MLU, Landesverwaltungsamt Sachsen-Anhalt). According to the FELASA guidelines, mice were housed in groups of up to 5 animals in a specific pathogen-free environment on a 12 h light/12 h dark cycle at 22 ± 2°C. The mice had free access to water and were fed a standard rodent diet (altromin) *ad libitum*. The cages were supplied with some paper towels as nesting material. Animal well-being was controlled daily. Mice which exceeded a previously determined welfare assessment score were killed immediately. At the end of the experiments, mice were killed by cervical dislocation.

In vivo matrigel plug assay

Sex-matched female and male vascular endothelial specific (cre-positive) TP knockout mice and cre-negative wild-type control littermates were subcutaneously injected with matrix containing endothelial cell growth media, methocel, fibrinogen, growth factors and high concentration matrigel (Corning, New York, USA) into the ventral region. After 7 days, mice were sacrificed and the matrigel plugs were removed and fixed with 4% PFA. The plugs were embedded in paraffin using standard protocols and cut into 6 µm thick sections. The neovessel formation was quantified after visualization of murine endothelial cells by FITC-labeled Griffonia simplicifolia lectin I (GSL I) isolectin B4 staining (1:100). Sections were co-stained with primary antibodies directed against murine hemoglobin (ab92492, abcam, 1:100 = 7.66 µg/mL). As a secondary antibody, Alexa Fluor 594-conjugated donkey-anti-rabbit (Jackson ImmunoResearch Laboratories) was used. Subsequent computer-aided histomorphometric analyses were performed using the NIS elements software package (Nikon). In addition, phenotypic characterization of the vascular network was done using antibody labelling of murine endothelial cell marker CD31 (Pecam-1; Santa Cruz Biotechnology; clone H3; 1:50 = 4 µg/mL). HRP-conjugated secondary antibodies were used as described by the manufacturer (Cell Signaling Technology, HRP-mouse (#8125)). For staining, we used the DAB-substrate kit according the manufacturer instructions (Cell Signaling Technology, #8059). A similar increase in VEGF- and bFGF-induced angiogenesis was observed in female and male vascular endothelial TP knockout mice as compared with wild-type littermates. Thus, to increase the power of our experiments and minimize the number of mice needed, we performed a pooled analysis of data from plugs obtained from male and female mice.

In vivo endothelial spheroid grafting assay

The EC spheroid-based grafting assay was performed as described previously [27, 28]. Spheroids were generated from stably transduced HUVEC and were subsequently embedded into a matrix containing endothelial cell growth media, methocel, fibrinogen,

growth factors and high concentration matrigel (Corning). Matrix and spheroids were injected subcutaneously into the ventral region of NSG™ mice. Mice were sacrified 21 days after implantation and plugs were explanted and fixed in 4% PFA. The plugs were embedded in paraffin using standard protocols and cut into 6 µm thick sections. The formation of humanoid neovessels were visualized by FITC-conjugated Ulex Europaeus Agglutinin I (UEA I, Vector Laboratories, California, USA) that specifically binds to human vascular endothelial cells. Sections were co-stained with primary antibodies directed against murine hemoglobin (ab92492, abcam, 1:100 = 7.66 µg/mL), as a secondary antibody Alexa Fluor 594-conjugated donkey-anti-rabbit (Jackson ImmunoResearch Laboratories) was used. Subsequent computer-aided histomorphometric analyzes using the NIS elements software package (Nikon) was performed for both stainings. For the visualization of murine endothelial cells, DyLight® 594-labeled Griffonia Simplicifolia Lectin I isolectin B4 (Vector Laboratories) was used. In addition, phenotypic characterization of the vascular network derived from HUVEC was performed by immunohistochemistry using antibody labelling of human endothelial cell markers CD31 (Cell Signaling Technology; clone 89C2; 1:750 = 33.5 ng/mL) and CD34 (Thermo Fisher Scientific; clone QBEnd/10; 1:500 = 2 µg/mL). HRP-conjugated secondary antibodies were used as described by the manufacturer (Cell Signaling Technology, HRP-Rabbit (#8114); HRP-mouse (#8125)). For staining, we used the DAB-substrate kit according the manufacturer instructions (Cell Signaling Technology, #8059). Separate analyses of histologically determined vessel density in female and male mice revealed that in both sexes, there was a similar trend towards increased blood vessel density with TP knockdown HUVEC and a trend towards decreased blood vessel density with TP-overexpressing HUVEC xenografts. Thus, to increase the power of our experiments and minimize the number of mice needed, we performed a pooled analysis of data from plugs obtained from male and female mice.

Statistical analyses

Two-group analysis of laminar flow-induced TP regulation, in which the respective single static control group value was set to 1 in each experiment, was performed using the Wilcoxon test. Two-group analyses of variables with skewed distribution were performed using the non-parametric Mann-Whitney U test as indicated, whereas the unpaired two-tailed Student's t-test was used for other two-group analyses. Multiple group analysis was performed using one-way analysis of variance followed by Sidak's multiple comparisons test except for multiple group analysis of variables with skewed distribution, which was performed using the Kruskal-Wallis test followed by Dunn`s test for multiple comparisons as indictated. For correlation analyses Spearman's rank correlation coefficient (Spearman's ρ) was used. All statistical analyses were performed using the Graph Pad Prism 6 software package (Graph Pad Software, Inc., La Jolla, USA). Data were expressed as mean ± standard deviation (SD), standard error of the mean (S.E.M.), or as indicated otherwise. Probability values were considered significant at a $p<0.05$.

Data availability

The data that support the findings of this study are available within the article and Supplemental files or from the corresponding author upon request. RNA-seq data that support the findings of this study have been deposited in the U.S. National Library of Medicine, National Center for Biotechnology Information Sequence Read Archive under accession code GSE146888.

Major Resources Table

Animals (in vivo studies)

Species	Vendor or Source	Background Strain	Sex	Persistent ID / URL
mouse	The Jackson Laboratory	NOD/ShiLtJ	m/f	#005557, URL
mouse	The Jackson Laboratory	129S6	m/f	#021985, URL
mouse	The Jackson Laboratory	C57BL/6J	m/f	#004128, URL

Genetically Modified Animals

	Species	Vendor or Source	Background Strain	Other Information	Persistent ID / URL
Parent - Male	mouse	The Jackson Laboratory	NOD/ShiLtJ	NOD-scid IL2rg^{null} (NSG^{TM})	# 005557, URL
Parent - Female	mouse	The Jackson Laboratory	NOD/ShiLtJ	NOD-scid IL2rg^{null} (NSG^{TM})	# 005557, URL
Parent – Male	mouse	The Jackson Laboratory	129S6	129S(Cg)-Tbxa2rtm1.1Bhk/J	#021985, URL
Parent – Female	mouse	The Jackson Laboratory	C57BL/6J	B6.Cg-Tg(Tek-cre)12Flv/J (TIE2Cre)	#004128, URL

Antibodies

Target antigen	Vendor or Source	Catalog #	Working concentration	Lot # (preferred but not required)	Persistent ID / URL
TPα	Cayman Chemical	10004452	1:500	-	URL
TPβ	Genscript	custom-made NP963998	1:500	-	**N/A**
Beta-Actin	Sigma Aldrich	A1978	1:5000 = 420 ng/mL	-	URL
Paxillin	abcam	ab32115	1.100 = 1.17 µg/mL	-	URL
Ki-67	Cell Signaling	9449	1:400 = 557.5 ng/mL	-	URL
Hemoglobin subunit alpha	abcam	ab92492	1:100 = 7.66 µg/mL	-	URL
CD31 (PECAM-1)	Cell Signaling	3528S	1:750 = 33.5 ng/mL	-	URL
CD31 (PECAM-1)	Santa Cruz Biotechnology	sc-376764	1:50 =4 µg/mL	-	URL
CD34	Thermo Fisher Scientific	MA1-10202	1:500 = 2 µg/mL	-	URL
COX-2	BD Pharmingen	565125	1:50 = 2 µg/mL	-	URL
VEGFR	BioLegend	359904	1:100 = 2 µg/mL	-	URL
DLL4	BioLegend	346508	1:100 = 4 µg/mL	-	URL

Mouse IgG1, κ Isotype Ctrl.	BioLegend	400113	1:50 = 2 µg/mL	-	URL

DNA/cDNA Clones

Clone Name	Sequence	Source / Repository	Persistent ID / URL
pHIV-SFiG-R135		Dr. Boris Fehse (Department of Stem Cell Transplantation, University Medical Center Hamburg-Eppendorf, Germany)	**N/A**
pHIV-TPα		Gene synthesis, subcloning into pHIV-SFiG-R135, GenScript	Custom made
pHIV-TPβ			
pHIV-RhoA Q63L			
pHIV-RhoA T19N			
pHIV-PTGIS			
LeGO-C2		Dr. Boris Fehse (Department of Stem Cell Transplantation, University Medical Center Hamburg-Eppendorf, Germany)	**N/A**
shTP1		GIPZ™ shRNA plasmids Horizon Discovery	#V3LHS_389249
shTP2			#V3LHS_389250
shPTGIR1			#RHS4430-200220940
shPTGIR2			#RHS4430-200223542
shGαq			#V3LHS_370027
shGα11			#V3LHS_306337
shCtr			#RHS4346
psPAX2		Addgene	#12260, URL
pMD2.G		Addgene	#12259, URL
Vinculin TS		Addgene	#26019, URL
Vinculin TL		Addgene	#26020, URL
Dora-RhoA FRET reporter (constitutive active, wildtype, dominant negative)		Dr. Yi I. Wu, (Center for cell analysis and Modeling, University of Connecticut Health Center, Farmington, United States of America)	**N/A**

Cultured Cells

Name	Vendor or Source	Sex (F, M, or unknown)	Persistent ID / URL
HUVEC	Lonza	unknown	C2519A, URL
HCAEC	Promocell	unknown	C-12221, URL
HAoEC	Lonza	unknown	CC-2535, URL

Data & Code Availability

Description	Source / Repository	Persistent ID / URL
RNA-Seq data	NCBI, Gene Expression Omnibus	GSE146888 / URL

Other

Description	Source / Repository	Persistent ID / URL
Hoechst 33342	life technologies	URL
Ulex europaeus agglutinin I (FITC-conjugated)	Vector laboratories	URL
Griffonia simplicifolia Lectin / Isolectin B4 (Rhodamine-conjugated	Vector laboratories	URL
Propidium Iodide	Sigma-Aldrich	URL
U-46619	Cayman Chemical	URL
SQ 29,548	Cayman Chemical	URL
VEGF-A	PeproTech	URL
bFGF	PeproTech	URL
Celecoxib	Santa Cruz Biotechnologie	**sc-217869**
Diclofenac	Santa Cruz Biotechnologie	URL
Ozagrel	Santa Cruz Biotechnologie	URL
Y-27632	Santa Cruz Biotechnologie	URL
BMS4	Axon Medchem	URL
(-)-Blebbistatin	Cayman Chemical	URL
Iloprost	Sigma Aldrich	URL
SiR actin	SpiroChrome	URL

Supplemental Figures

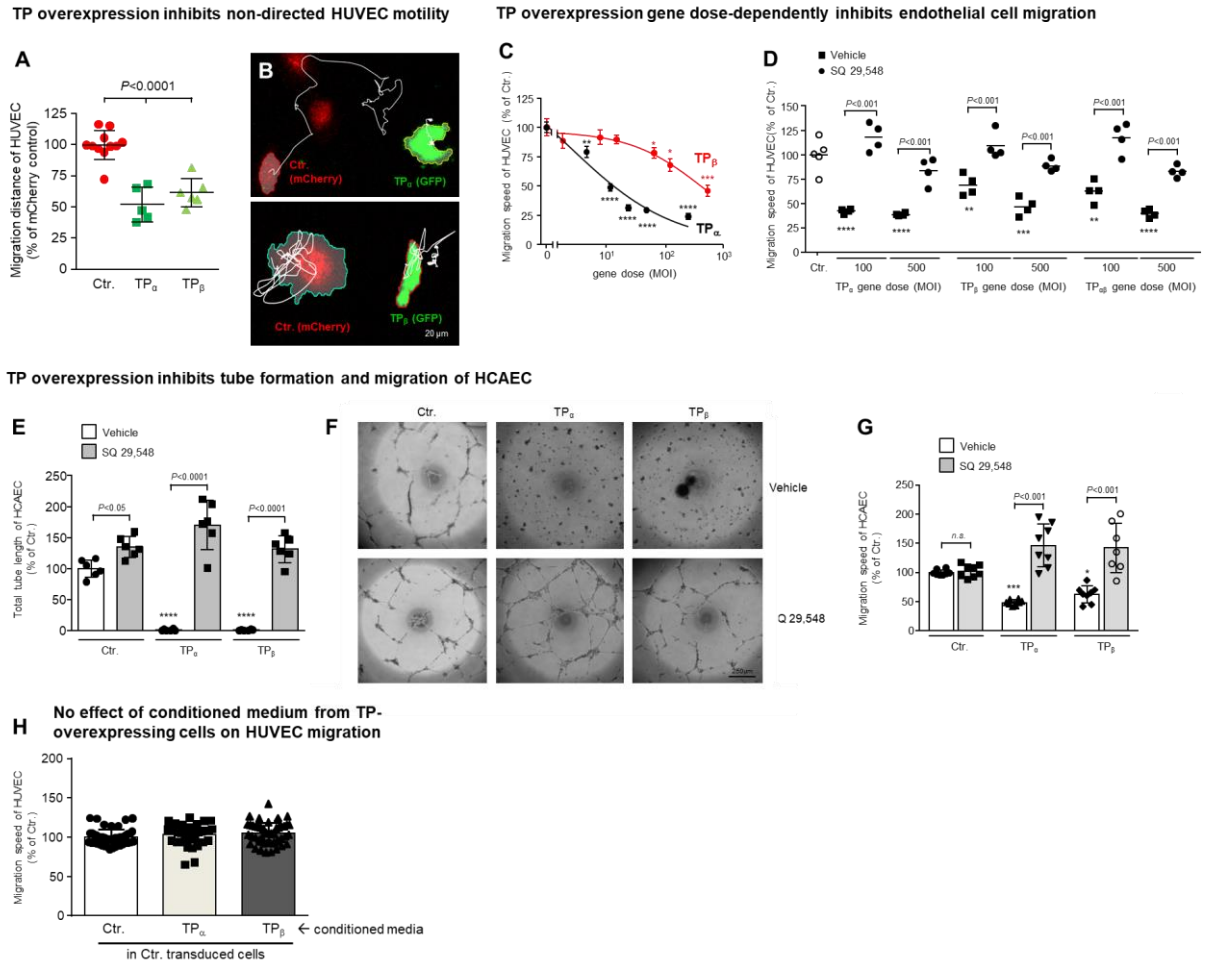

Figure S1. A,B) Overexpression of either TP_α or TP_β in HUVEC significantly reduces non-directed motility of these cells as evidenced by concomitant live-cell imaging of mCherry-tagged control cells and TP_α- or TP_β-overexpressing endothelial cells co-expressing the fluorescent reporter EGFP (n=5-10). B) Representative plots depict the individual migration distance (fine lines) during the observational period covered by TP-overexpressing or control cells. C) Overexpression of either TP_α or TP_β inhibits migration speed of HUVEC in a gene dose dependent manner. MOI (multiplicity of infection) represents a measure of the count of viral particles delivered to one single cell. D) Migration speed of HUVEC overexpressing TP_α only, TP_β only or both TP isoforms in two different gene doses (MOI 100 and 500), respectively. The reduction in migration speed of TP-overexpressing cells is reversed by the TP antagonist SQ 29,548 ($3x10^{-5}$ mol/L). All statistical analyses in Figure S1 were performed using one-way analysis of variance followed by Sidak's multiple comparisons test. * $p<0.05$ / ** $p<0.01$ / *** $p<0.001$ / **** $p<0.0001$ vs. control-transduced HUVEC (n=4-5). E-G) Overexpression of either TP_α or TP_β inhibits tube formation (E,F) or scratch-induced migration (G) of human coronary artery endothelial cells (HCAEC). This effect is reversed by

pharmacological TP inhibition (SQ-29548; $3x10^{-5}$ mol/L). * $p<0.05$ / *** $p<0.001$ / **** $p<0.0001$ vs. control-transduced HCAEC (n=7-8). H) Conditioned medium derived from control (Ctr.) and TP_{α}- or TP_{β}-overexpressing HUVEC, respectively, did not affect migration speed of native HUVEC.

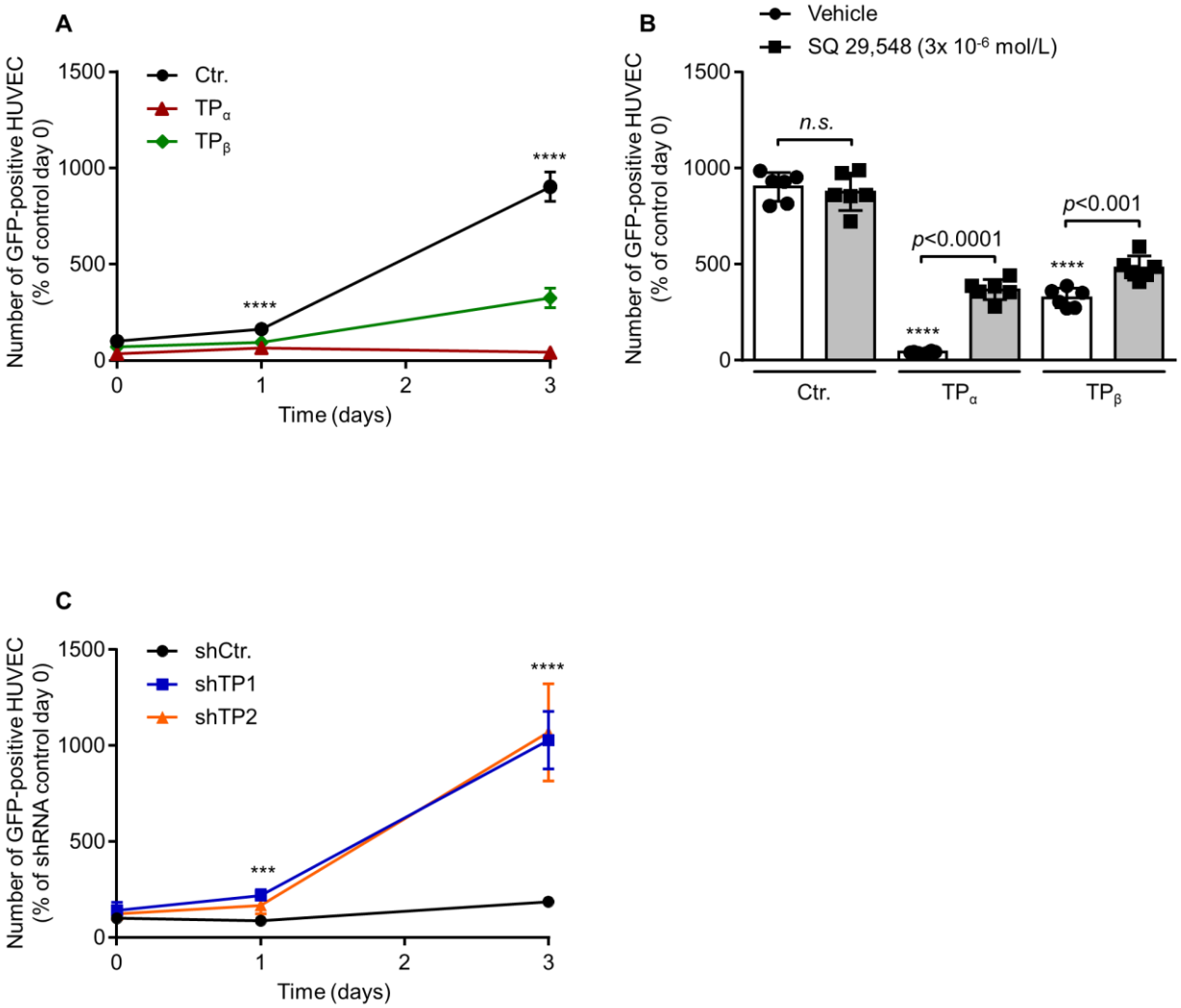

Figure S2. Flow cytometric analysis of lentivirally transduced GFP-positive HUVEC shows that the TP inhibits HUVEC proliferation under two-dimensional culture conditions *in vitro*. A) Both TP_{α} and TP_{β} overexpression inhibit proliferation of HUVEC. Data are expressed as mean ± SD. (n=6), **** $p<0.0001$ of Ctr. vs. either TP_{α} or TP_{β}. All statistical analyses in Figure S2 were performed using the one-way analysis of variance followed by Sidak's multiple comparisons test. B) The pharmacological TP antagonist SQ 29,548 ($3x10^{-6}$ mol/L) attenuates the inhibitory effect of both TP isoforms as determined 3 days after plating of the cells. (n=6), **** $p<0.0001$ vs. Ctr. C) In contrast, knockdown of the TP using two different shRNAs (shTP1, shTP2) strongly induces HUVEC proliferation in this set-up. Data are expressed as mean ± SD. (n=6), **** $p<0.0001$ vs. shCtr.

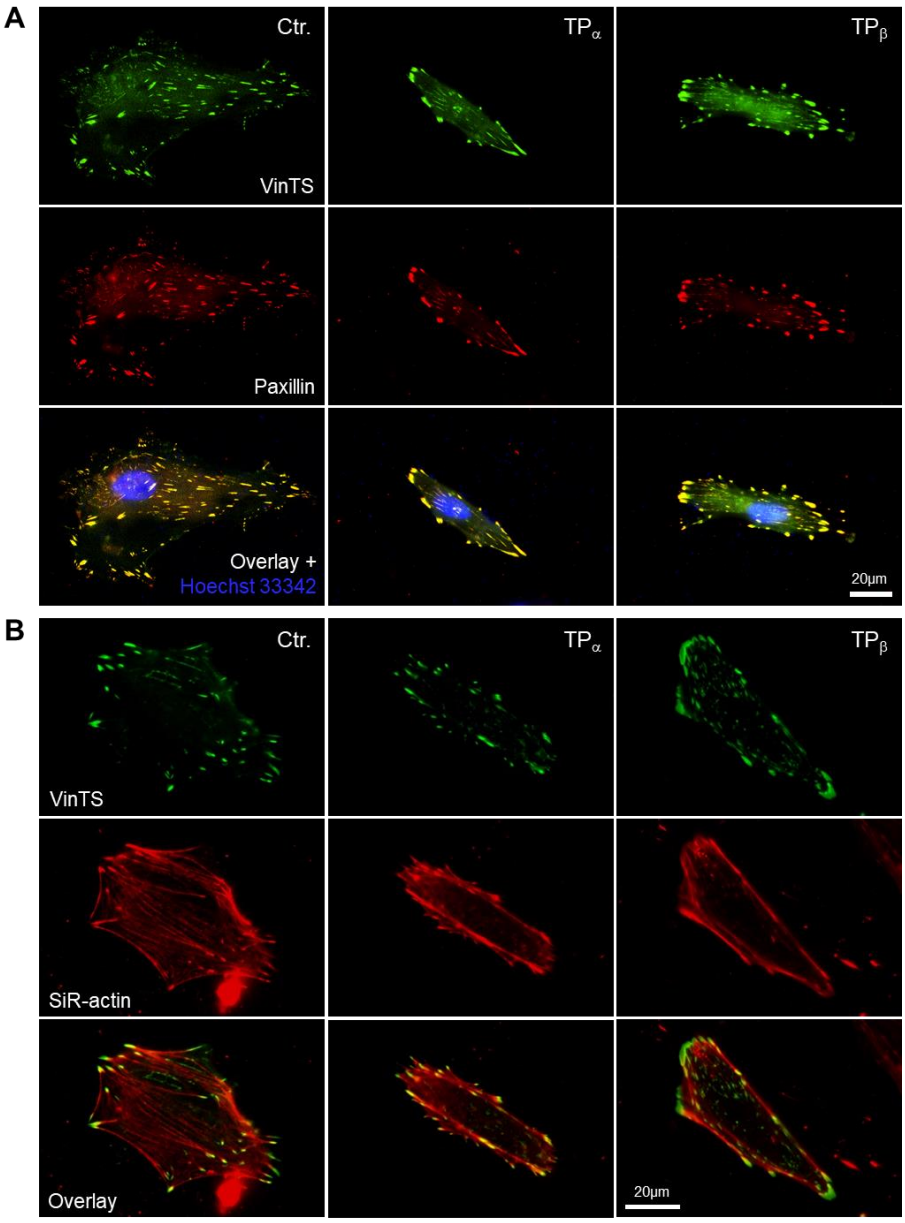

Figure S3. Colocalization of VinTS with paxillin and association of VinTS-positive focal adhesions with actin stress fibers. A) TP-overexpressing (TP_α, TP_β) as well as appropriate control HUVEC (Ctr.) were transfected with vinculin tension sensor (VinTS), then fixed and stained with antibodies directed against the focal adhesion marker paxillin. In all condition, VinTS and paxillin colocalized, indicating that VinTS expression is restricted to focal adhesions. In TP_α– and TP_β-overexpressing HUVEC, a marked cortical localization of focal adhesions was observed. B) HUVEC transfected with VinTS were stained with the live-cell actin-labeling dye SiR-actin. In control cells (Ctr.), actin fibers spread throughout the cell and were associated with focal adhesions (VinTS). In contrast, in HUVEC overexpressing TP_α or TP_β, both focal adhesions and actin stress fibers, which again associated with the focal adhesions, were localized particularly at the cell margin.

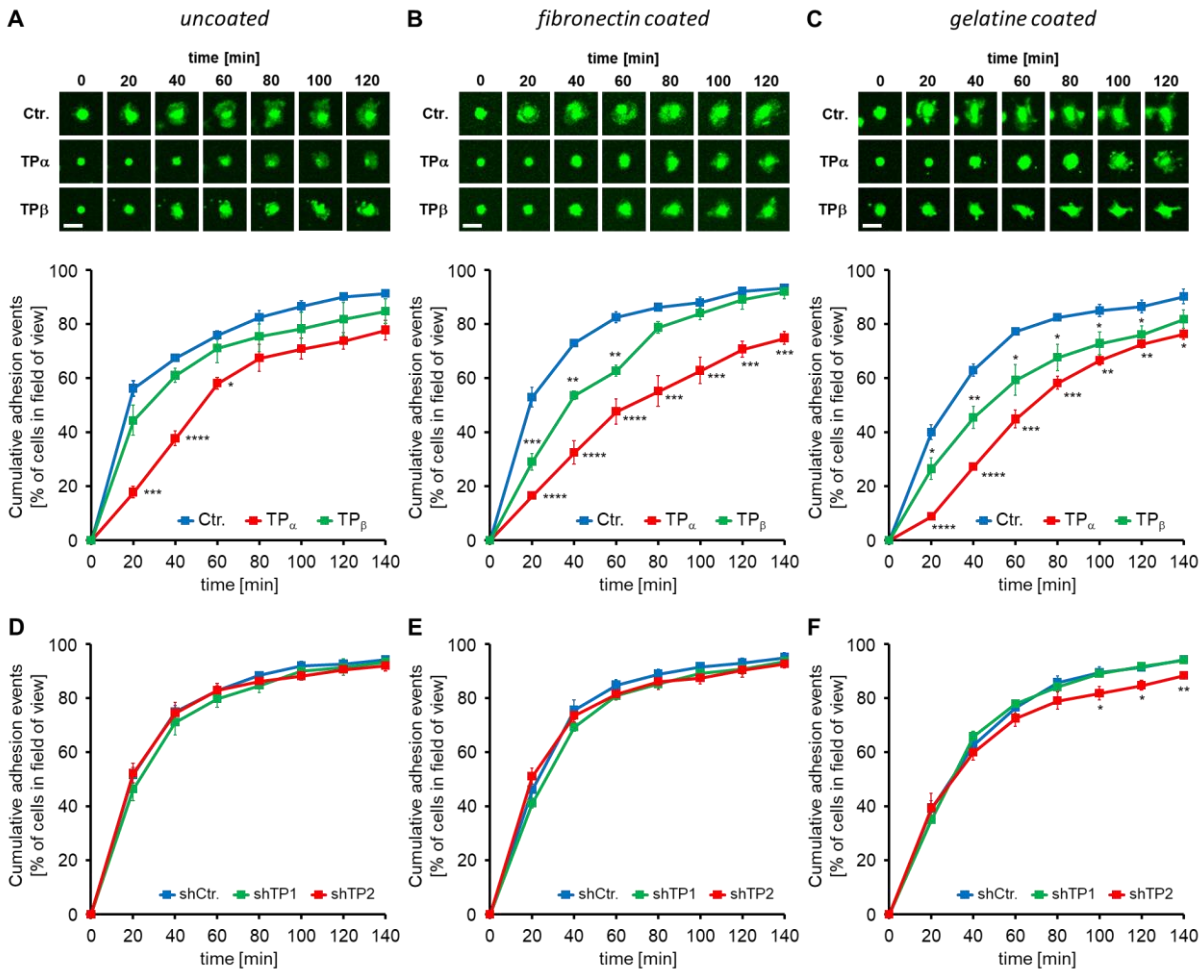

Figure S4. TP overexpression decelerates adhesion of human endothelial cells. Time lapse video microscopy of HUVEC transduced with lentiviral particles (Ctr., TP_{α}, TP_{β}) after being seeded on differently coated surfaces (A: uncoated, B: fibronectin-coated, C: gelatine-coated). Representative pictures show time-lapse recordings of individual cells during the cell adhesion process. The total number of cell attachment events to the surface within the field of view was counted for each time frame and normalized to the total number of cells. As shown in the statistical analyses of cumulative adhesion events, overexpression of in particular TP_{α} and of TP_{β} significantly delayed adhesion of the cells to the surface. The effect was most pronounced on fibronectin- and gelatine-coated surfaces. D-F) In contrast, TP knockdown did not consistently alter the adhesiveness of HUVEC on differently coated surfaces. Scalebar = 50µm, * $p<0.05$ / ** $p<0.01$ / *** $p<0.001$ / **** $p<0.0001$ vs. control-transduced HUVEC (n=4), One-way analysis of variance followed by Sidak's multiple comparisons test.

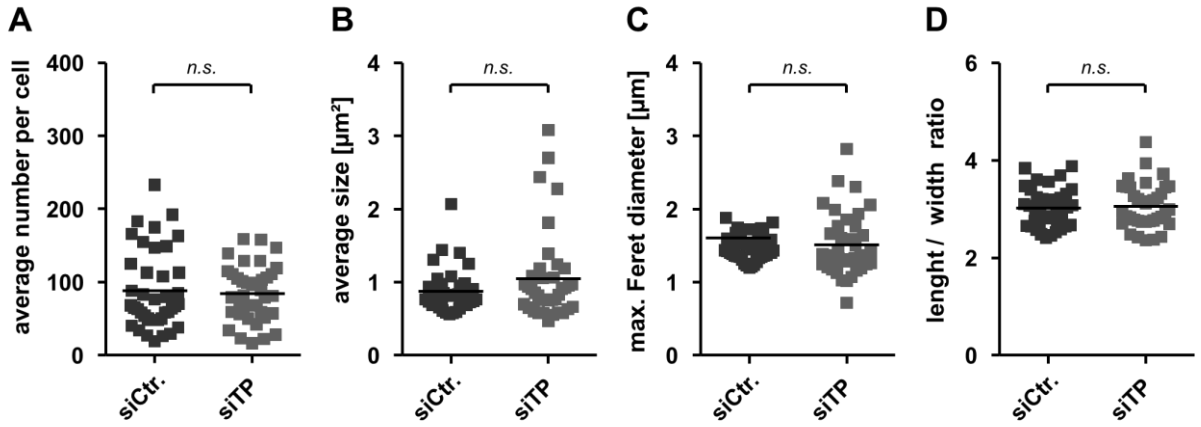

Figure S5. TP knockdown has no significant effect on focal adhesion morphology. Focal adhesions of HUVEC transfected with siRNA directed against the TP (siTP) or control siRNA (siCtr.) were imaged and analysed for changes of focal adhesion morphology. n.s. = not significant, unpaired two-tailed Student's t-test.

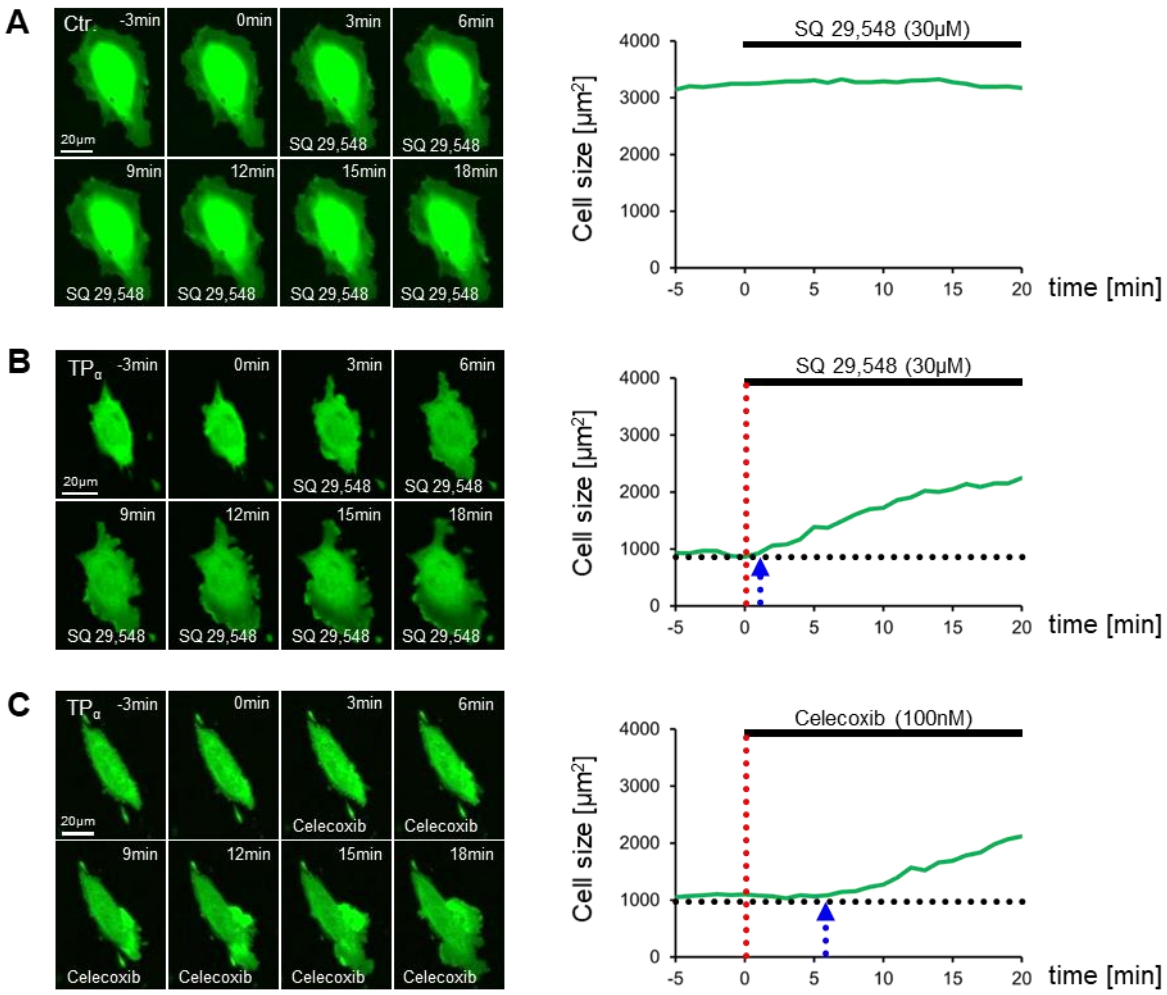

Figure S6. Increased TP expression induces endothelial cell contraction. A-C) Expansion of TP-overexpressing cells after addition of the TP antagonist SQ 29,548 ($3x10^{-5}$ mol/L; A-B) or the COX-2 inhibitor celecoxib (100 nmol/L; C). Control-transduced (Ctr.; A) or TP_{α}-overexpressing (TP_{α}; B and C) HUVEC additionally expressing mVenus. Black dotted lines denote the approximate cell size before the addition of the respective pharmacological antagonist. Addition of the respective antagonist (time point "0") is indicated by red dotted lines. Blue arrows denote the approximate beginning of SQ 29,548- or celecoxib-induced endothelial cell expansion in TP_{α}-overexpressing HUVEC.

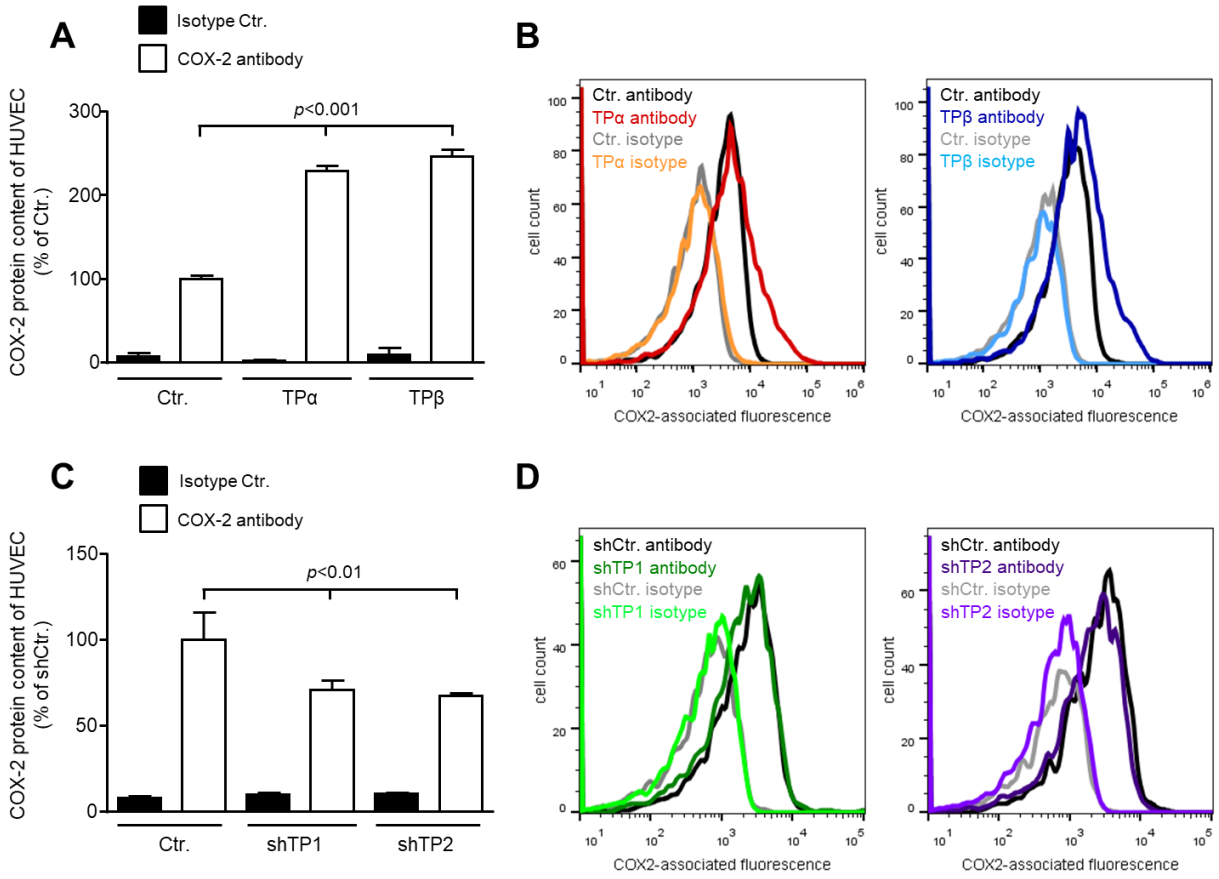

Figure S7. Flow cytometric analyses demonstrate that the TP is a positive regulator of COX-2 content in HUVEC. A and B) Overexpression of both TP_{α} and TP_{β} increases COX-2 protein content in HUVEC, whereas it does not affect isotype control-associated fluorescence in these cells. In contrast, shRNA-mediated knockdown of the TP using two different shRNAs (shTP1, shTP2; C and D) significantly reduces COX-2 protein levels in HUVEC and again does not affect isotype control-associated fluorescence in this set up. B and D) Representative flow cytometric plots depicting TP-induced changes in COX-2-associated fluorescence (Ab = antibody; Isotype = isotype control). Data are shown as mean ± SD (n=3). All statistical analyses in Figure S7 were performed using one-way analysis of variance followed by Sidak's multiple comparisons test.

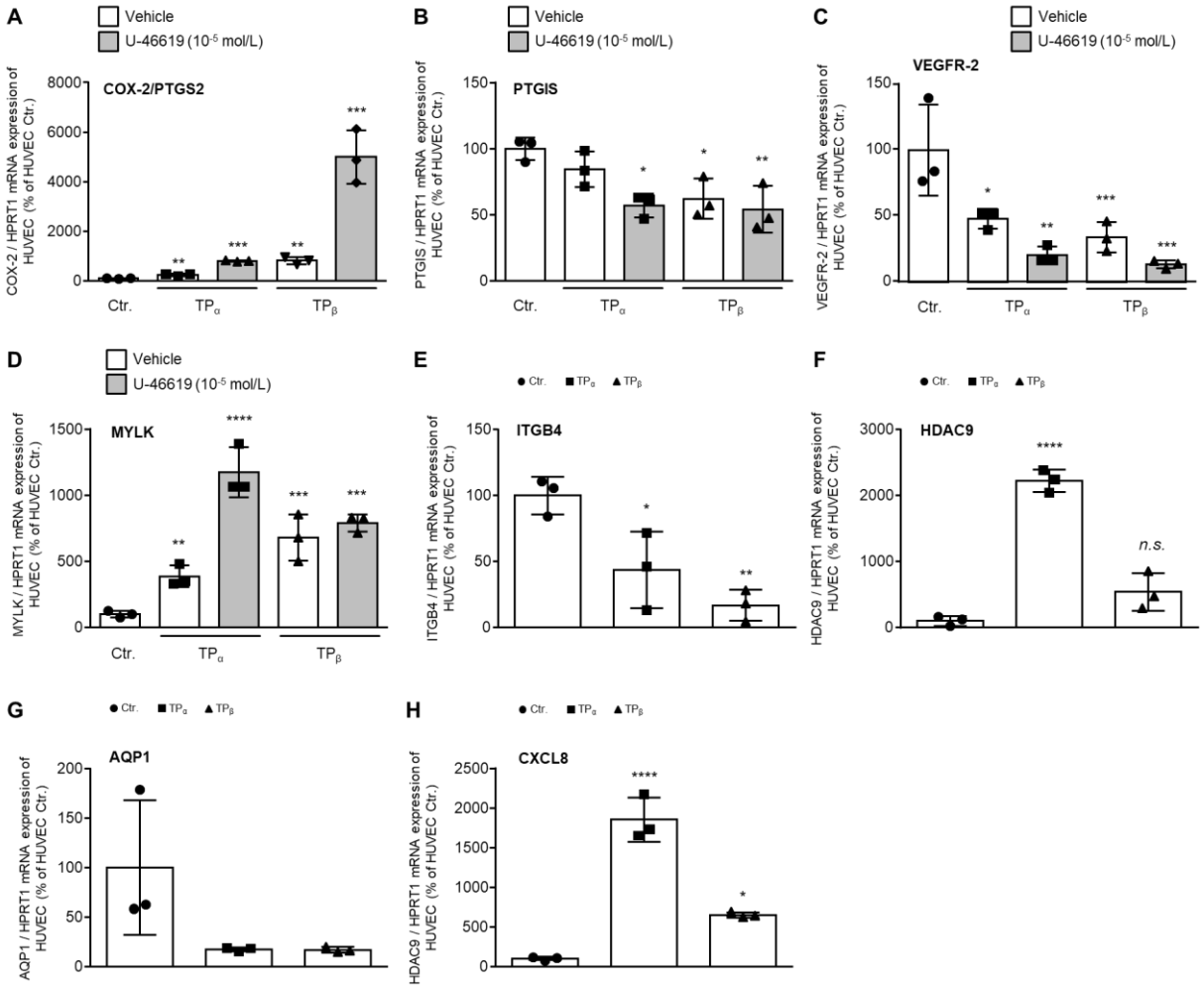

Figure S8. A-H) Validation of RNA-Seq results of selected genes using qRT-PCR. * p<0.05 / ** p<0.01 / *** p<0.001 / **** p<0.0001 vs. control-transduced HUVEC (n=3). The statistical analyses in Figure S8 were performed using one-way analysis of variance followed by Sidak's multiple comparisons test.

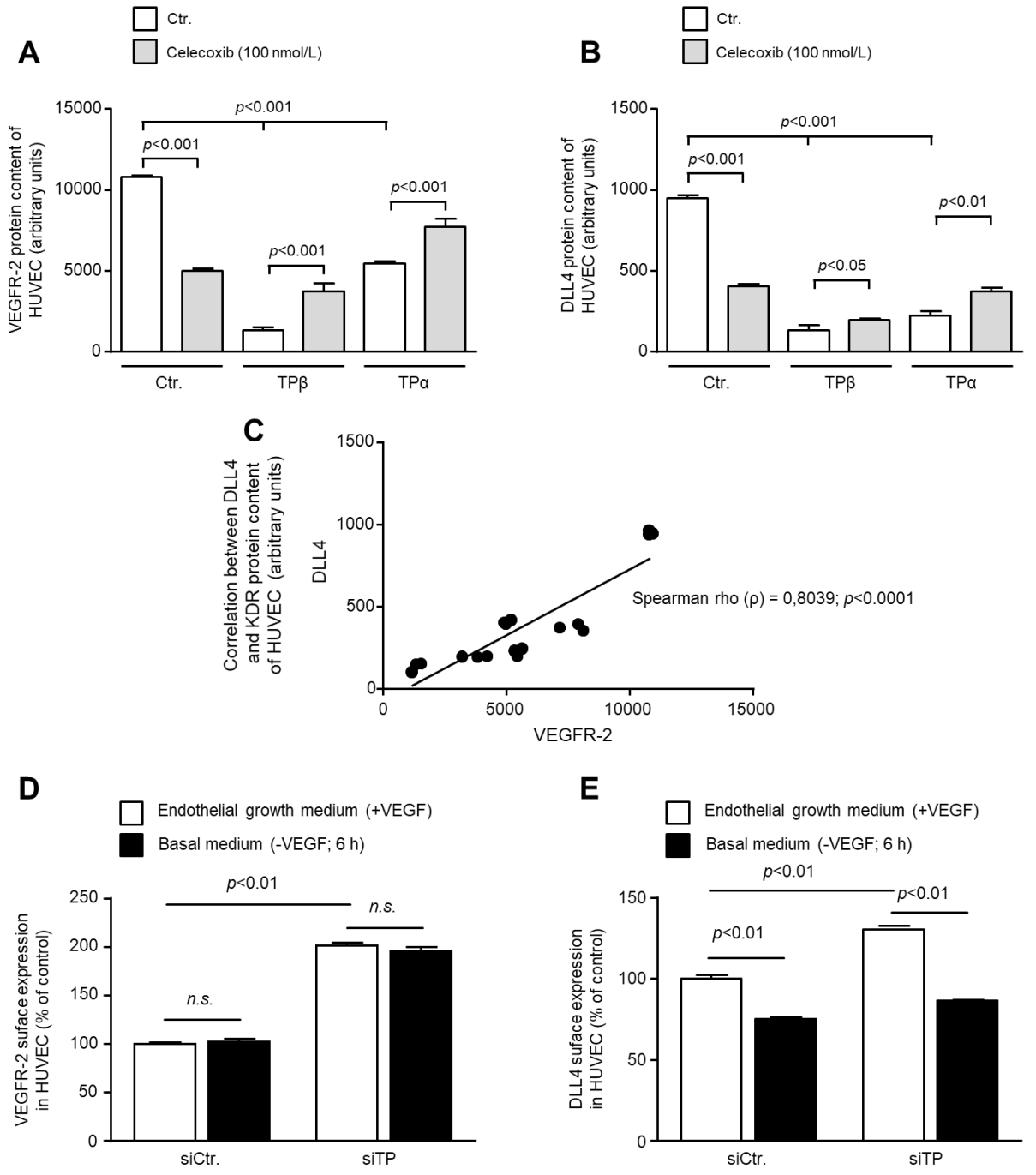

Figure S9. The TP is a negative regulator of VEGFR-2 and DLL4 expression in HUVEC. A and B) TP_{α} and TP_{β} overexpression reduce VEGFR-2 as well as DLL4 protein levels as detected by flow cytometry in HUVEC (n=3). COX-2 inhibitor celecoxib (100 nmol/L) significantly attenuates TP overexpression-induced downregulation of both VEGFR-2 and DLL4, whereas in control cells it reduces VEGFR-2 and DLL4 expression (n=3). Statistical analyses in Figure S9A,B,D,E were performed using the one-way analysis of variance followed by Sidak's multiple comparisons test. Furthermore, we observed a strong positive correlation between VEGFR-2 and DLL4 expression in HUVEC grown in VEGF-containing medium, supporting the mechanistic concept that DLL4 expression is dependent on VEGFR-

2 activity in human endothelial cells. For correlation analyses Spearman's rank correlation coefficient (Spearman's ρ) was used. D-E) TP knockdown increases both VEGFR-2 and DLL4 expression in HUVEC. In this context, VEGF withdrawal from the medium does not affect TP knockdown-induced VEGFR-2 upregulation but completely abolishes DLL4 upregulation in TP knockdown cells (E).

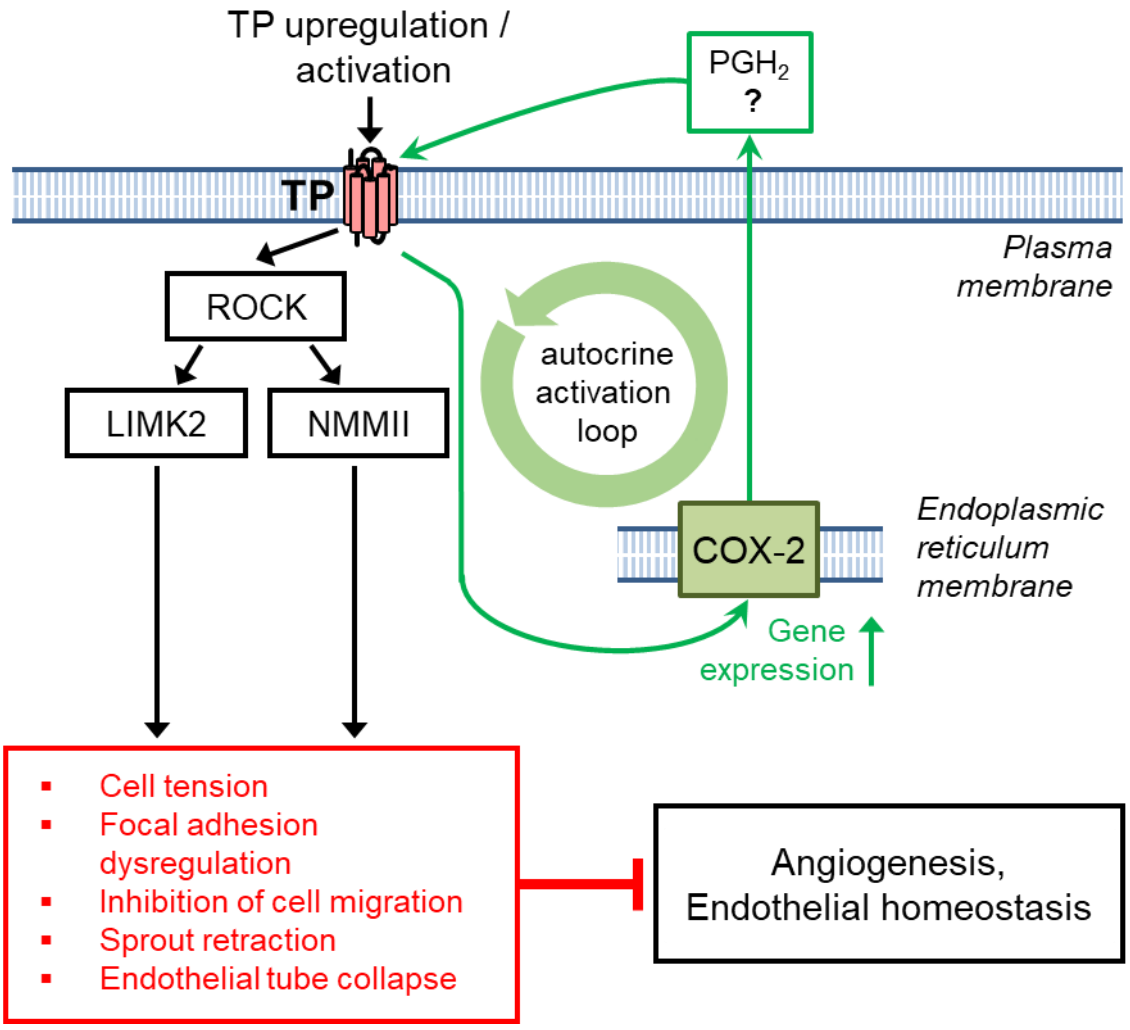

Figure S10. Schematic representation of the TP-driven anti-angiogenic feedback loop in vascular endothelial cells. This feedback loop involves a TP-dependent COX-2 upregulation and consecutive persistent TP activation most likely by enhanced biosynthesis of the short-lived TP agonist PGH_2 or other TP-agonistic prostanoids such as $PGF_{2\alpha}$. Subsequently, TP-dependent activation of a ROCK-LIMK2-myosin II-dependent signal transduction pathway increases cell tension, disturbs focal adhesion dynamics and inhibits endothelial cell migration, tube formation and sprouting.

Supplemental Video Legends

Video S1

Live-cell imaging of two-dimensional endothelial cell migration reveals that TP overexpression *per se* (both the TP_{α} and TP_{β} isoform, green cells) strongly affects HUVEC motility and cell proliferation as compared to mCherry-expressing control cells (red cells). TP overexpression induces an elongated, branched cellular phenotype with irregularly shaped lamellipodia and cell extensions.

Video S2

Live-cell imaging of scratch-induced two-dimensional endothelial cell migration using the scratch assay shows that TP_{α} overexpression *per se* severely impairs endothelial cell motility of HUVEC. TP overexpression-related inhibition of endothelial cell migration is antagonized by pharmacological inhibition of the TP using the TP antagonist SQ 29,548 ($3x10^{-5}$ mol/L).

Video S3

Control spheroids, consisting of GFP- and mCherry-expressing control HUVEC, show the dynamic formation of a balanced and regular sprout morphology during stimulation with VEGF (20 ng/mL), thereby revealing typical characteristics of angiogenic sprout formation, i.e. tip and stalk cell competition. However, TP overexpression, in the absence of exogenous TP agonists, markedly inhibits VEGF-induced sprouting from HUVEC spheroids. TP-overexpressing HUVEC (green cells) in tip cell position show extensive retraction and early collapse of angiogenic sprouts leading to an early demise of the sprouts. Moreover, TP-overexpressing HUVEC in stalk cell position apparently exert considerable tractional forces during their interaction with (red) control HUVEC leading to retraction of mature (control HUVEC-derived) sprouts and deformation of the endothelial spheroid.

Video S4

Pharmacological inhibition of the TP (SQ 29,548, $3x10^{-5}$ mol/L) or cyclooxygenase-2 (celecoxib, 100 nmol/L) but not solvent control reduces vascular endothelial cell

tension in TP_β-overexpressing HUVEC as indicated by an increase in FRET efficiency of the VinTS biosensor after addition of the inhibitors.

Video S5

The TP antagonist SQ 29,548 ($3x10^{-5}$ mol/L) and the cyclooxygenase-2 inhibitor celecoxib (100 nmol/L) support the disassembly of focal adhesions in TP_β-overexpressing HUVEC in two-dimensional cell culture. Focal adhesion dynamics were visualized by additionally transfecting HUVEC with the vinculin-based tension biosensor (VinTS). mVenus fluorescence intensity of VinTS is visualized in a false colour-coded fashion ranging from light yellow (high intensity) to blue (low intensity).

Supplemental Data Set Legends

File Name: Data Set 1

Description: RNA-seq data showing differentially expressed genes in TP_{α}-overexpressing (TP_{α} value) HUVEC as compared to appropriate control HUVEC (Control value).

File Name: Data Set 2

Description: RNA-seq data showing differentially expressed genes in TP_{β}-overexpressing (TP_{β} value) HUVEC as compared to appropriate control HUVEC (Control value).

File Name: Data Set 3

Description: A detailed heat map including gene annotations showing the results of hierarchical clustering of TP overexpression-related differentially expressed genes using FPKM as the input.

References

1. Grashoff C, Hoffman BD, Brenner MD, Zhou R, Parsons M, Yang MT, McLean MA, Sligar SG, Chen CS, Ha T, Schwartz MA. Measuring mechanical tension across vinculin reveals regulation of focal adhesion dynamics. *Nature*. 2010;466:263-266
2. Lin B, Yin T, Wu YI, Inoue T, Levchenko A. Interplay between chemotaxis and contact inhibition of locomotion determines exploratory cell migration. *Nat Commun*. 2015;6:6619
3. van Unen J, Reinhard NR, Yin T, Wu YI, Postma M, Gadella TW, Goedhart J. Plasma membrane restricted rhogef activity is sufficient for rhoa-mediated actin polymerization. *Sci Rep*. 2015;5:14693
4. Reinhard NR, van Helden SF, Anthony EC, Yin T, Wu YI, Goedhart J, Gadella TW, Hordijk PL. Spatiotemporal analysis of rhoa/b/c activation in primary human endothelial cells. *Sci Rep*. 2016;6:25502
5. Tiscornia G, Singer O, Verma IM. Production and purification of lentiviral vectors. *Nat Protoc*. 2006;1:241-245
6. Kutner RH, Zhang XY, Reiser J. Production, concentration and titration of pseudotyped hiv-1-based lentiviral vectors. *Nat Protoc*. 2009;4:495-505
7. Korff T, Augustin HG. Integration of endothelial cells in multicellular spheroids prevents apoptosis and induces differentiation. *J Cell Biol*. 1998;143:1341-1352
8. Liang CC, Park AY, Guan JL. In vitro scratch assay: A convenient and inexpensive method for analysis of cell migration in vitro. *Nat Protoc*. 2007;2:329-333
9. Benndorf RA, Schwedhelm E, Gnann A, Taheri R, Kom G, Didié M, Steenpass A, Ergün S, Böger RH. Isoprostanes inhibit vascular endothelial growth factor-induced endothelial cell migration, tube formation, and cardiac vessel sprouting in vitro, as well as angiogenesis in vivo via activation of the thromboxane a(2) receptor: A potential link between oxidative stress and impaired angiogenesis. *Circ Res*. 2008;103:1037-1046
10. Deppe S, Ripperger A, Weiss J, Ergün S, Benndorf RA. Impact of genetic variability in the abcg2 gene on abcg2 expression, function, and interaction with at1 receptor antagonist telmisartan. *Biochem Biophys Res Commun*. 2014;443:1211-1217
11. Weil J, Benndorf R, Fredersdorf S, Griese DP, Eschenhagen T. Norepinephrine upregulates vascular endothelial growth factor in rat cardiac myocytes by a paracrine mechanism. *Angiogenesis*. 2003;6:303-309
12. Weiss J, Sauer A, Herzog M, Böger RH, Haefeli WE, Benndorf RA. Interaction of thiazolidinediones (glitazones) with the atp-binding cassette transporters p-glycoprotein and breast cancer resistance protein. *Pharmacology*. 2009;84:264-270
13. Livak KJ, Schmittgen TD. Analysis of relative gene expression data using real-time quantitative pcr and the 2(-delta delta c(t)) method. *Methods*. 2001;25:402-408
14. Ripperger A, Benndorf RA. The c421a (q141k) polymorphism enhances the 3'-untranslated region (3'-utr)-dependent regulation of atp-binding cassette transporter abcg2. *Biochem Pharmacol*. 2016;104:139-147
15. Kim D, Langmead B, Salzberg SL. Hisat: A fast spliced aligner with low memory requirements. *Nat Methods*. 2015;12:357-360
16. Yates A, Akanni W, Amode MR, et al. Ensembl 2016. *Nucleic Acids Res*. 2016;44:D710-716
17. Trapnell C, Williams BA, Pertea G, Mortazavi A, Kwan G, van Baren MJ, Salzberg SL, Wold BJ, Pachter L. Transcript assembly and quantification by rna-seq reveals unannotated transcripts and isoform switching during cell differentiation. *Nat Biotechnol*. 2010;28:511-515

18. Love MI, Huber W, Anders S. Moderated estimation of fold change and dispersion for rna-seq data with deseq2. *Genome Biol*. 2014;15:550
19. Young MD, Wakefield MJ, Smyth GK, Oshlack A. Gene ontology analysis for rna-seq: Accounting for selection bias. *Genome Biol*. 2010;11:R14
20. Werner M, Jordan PM, Romp E, Czapka A, Rao Z, Kretzer C, Koeberle A, Garscha U, Pace S, Claesson HE, Serhan CN, Werz O, Gerstmeier J. Targeting biosynthetic networks of the proinflammatory and proresolving lipid metabolome. *Faseb j*. 2019;33:6140-6153
21. Werz O, Gerstmeier J, Libreros S, De la Rosa X, Werner M, Norris PC, Chiang N, Serhan CN. Human macrophages differentially produce specific resolvin or leukotriene signals that depend on bacterial pathogenicity. *Nat Commun*. 2018;9:59
22. Koeberle A, Munoz E, Appendino GB, Minassi A, Pace S, Rossi A, Weinigel C, Barz D, Sautebin L, Caprioglio D, Collado JA, Werz O. Sar studies on curcumin's pro-inflammatory targets: Discovery of prenylated pyrazolocurcuminoids as potent and selective novel inhibitors of 5-lipoxygenase. *J Med Chem*. 2014;57:5638-5648
23. Gehling UM, Willems M, Schlagner K, Benndorf RA, Dandri M, Petersen J, Sterneck M, Pollok JM, Hossfeld DK, Rogiers X. Mobilization of hematopoietic progenitor cells in patients with liver cirrhosis. *World J Gastroenterol*. 2010;16:217-224
24. Cyphert JM, Allen IC, Church RJ, Latour AM, Snouwaert JN, Coffman TM, Koller BH. Allergic inflammation induces a persistent mechanistic switch in thromboxane-mediated airway constriction in the mouse. *Am J Physiol Lung Cell Mol Physiol*. 2012;302:L140-151
25. Koni PA, Joshi SK, Temann UA, Olson D, Burkly L, Flavell RA. Conditional vascular cell adhesion molecule 1 deletion in mice: Impaired lymphocyte migration to bone marrow. *J Exp Med*. 2001;193:741-754
26. King MA, Covassin L, Brehm MA, et al. Human peripheral blood leucocyte non-obese diabetic-severe combined immunodeficiency interleukin-2 receptor gamma chain gene mouse model of xenogeneic graft-versus-host-like disease and the role of host major histocompatibility complex. *Clin Exp Immunol*. 2009;157:104-118
27. Laib AM, Bartol A, Alajati A, Korff T, Weber H, Augustin HG. Spheroid-based human endothelial cell microvessel formation in vivo. *Nat Protoc*. 2009;4:1202-1215
28. Braun H, Hauke M, Ripperger A, Ihling C, Fuszard M, Eckenstaler R, Benndorf RA. Impact of dicer1 and drosha on the angiogenic capacity of human endothelial cells. *Int J Mol Sci*. 2021;22